Supporting information

Catalytic Activity of Bimetallic Catalysts Highly Sensitive to Atomic Composition and Phase Structure at the Nanoscale

Shiyao Shan,[a] Valeri Petkov,[b,*] Binay Prasai,[b] Jinfang Wu,[a] Pharrah Joseph,[a] Zakiya Skeete[a], Eunjoo Kim,[a] Derrick Mott,[c] Oana Malis,[d] Jin Luo,[a] and Chuan-Jian Zhong,[a,*]

[a)] Department of Chemistry, State University of New York at Binghamton, Binghamton, NY 13902, USA
[b)] Department of Physics, Central Michigan University, Mt. Pleasant, Michigan 48859, USA
[c)] School of Materials Science, Japan Advanced Institute of Science and Technology, 1-1 Asahidai, Nomi, 923-1292 Ishikawa, Japan.
[d)] Department of Physics, Purdue University, West Lafayette, IN, USA
(* To whom correspondence should be addressed. Emails: cjzhong@binghamton.edu, and petko1vg@cmich.edu))

Additional Experimental Data:

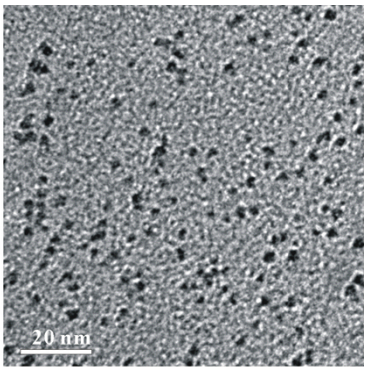

Figure S1. A representative TEM image for a sample of as-synthesized (E-) $Pd_{58}Cu_{42}$ nanoparticles.

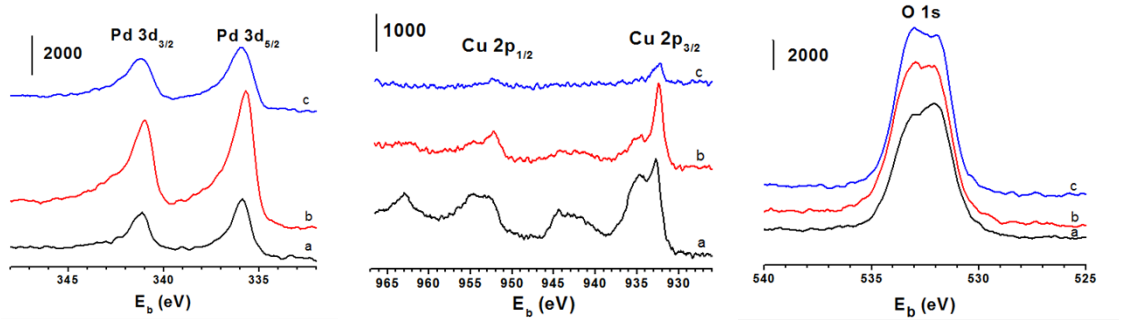

(A) (B) (C)

Figure S2. XPS spectra of carbon-supported (B-) $Pd_{21}Cu_{79}/C$ (black, a), $Pd_{48}Cu_{52}/C$ (red, b) and $Pd_{75}Cu_{25}/C$ (blue, c) in regions of Pd 3d(A), Cu 2p(B) and O 1s (D)

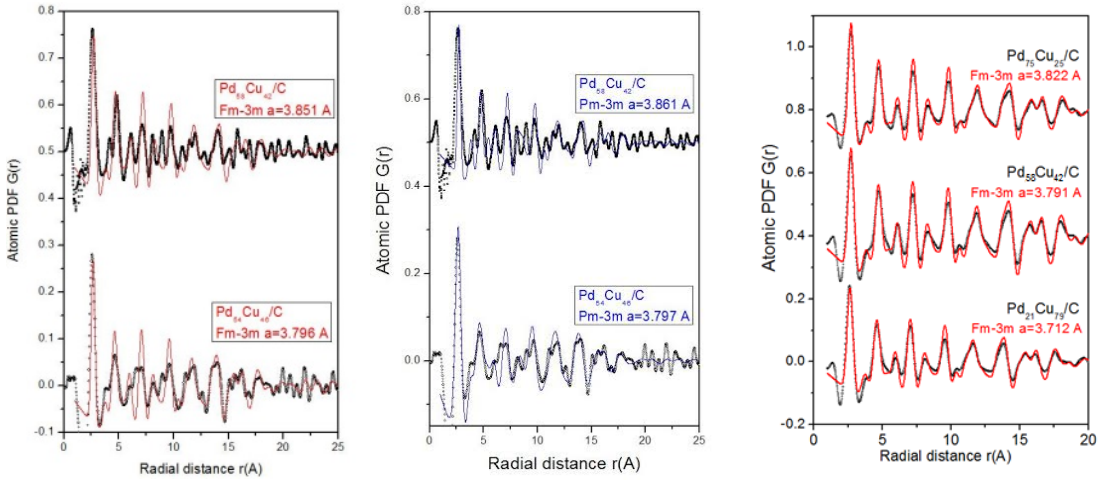

(A) (B) (C)

Figure S3. Experimental (black symbols) and fcc model (A, line in red) and bcc model (B, line in blue) atomic PDFs for both (E-) $Pd_{58}Cu_{42}$/C (top) and (B-) $Pd_{54}Cu_{46}$/C (bottom) under H_2 at 200 °C. Model PDFs were fitted with both a chemically disordered alloy with a fcc-type (Fm-3m) structure and a chemically ordered alloy with a bcc-type (Pm-3m) structure. Refined fcc lattice parameters and bcc lattice parameters are shown by each data set. (C) Experimental (symbols) and model (line in red) atomic PDFs for fresh $Pd_{25}Cu_{75}$/C, $Pd_{58}Cu_{42}$/C and $Pd_{77}Cu_{23}$/C alloy NPs which were treated under O_2 at 260 °C followed by H_2 at 400 °C. Model PDFs feature a chemically disordered alloy with a fcc-type (Fm-3m) structure. Refined fcc lattice parameters are shown by each data set.

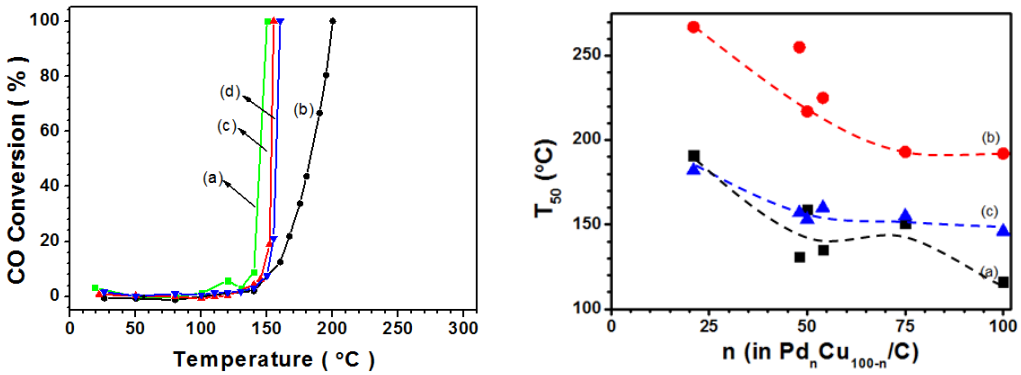

(A) (B)

Figure S4. (A) CO oxidation activities for Pd (green, a), $Pd_{21}Cu_{79}$ (black, b), $Pd_{48}Cu_{52}$ (red, c), and $Pd_{75}Cu_{25}$ (blue, d) catalysts in reduced (treated under H_2) state and (B) T_{50} values as a function of the bimetallic composition comparing (1) fresh catalysts (a, black); (2) catalysts oxidized under O_2 at 450 °C for 30min (b, red); and (3) catalysts reduced under H_2 at 300 °C for 30 min (c, blue).

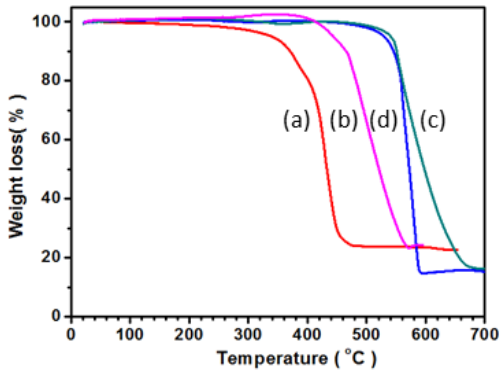

Figure S5. TGA curves for Cu/C (a, red) , $Pd_{21}Cu_{79}$/C (b, purple), $Pd_{54}Cu_{46}$/C (c, dard green), and $Pd_{75}Cu_{25}$/C (d, blue) catalysts under 30% O_2 at the flow rate of 130 ml/min.

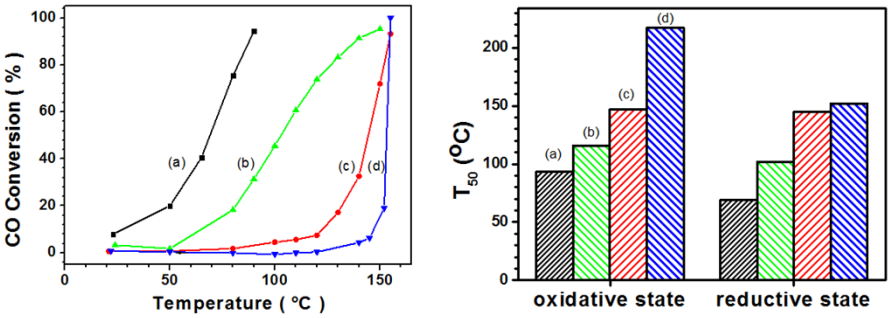

(A) (B)

Figure S6. (A) CO oxidation activities for reduced $Pd_{48}Cu_{52}$ alloy NPs on different support: TiO_2 (a, black); CeO_2 (b, green), SiO_2 (c, red), and carbon (d, blue) and (B) T_{50} values for $Pd_{48}Cu_{52}$ catalysts over different supports (i.e. TiO_2 (a, black), CeO_2 (b, green), SiO_2 (c, red), and Carbon (d, blue)) initially treated at 260 °C under N_2 and then under reductive under 15 vol. % H_2 at 400 °C followed by further treatment either under O_2 at 450 °C for 30 min, denoted on the plot as oxidative state, or under H_2 at 300 °C for 30 min, denoted on the plot as reductive state.

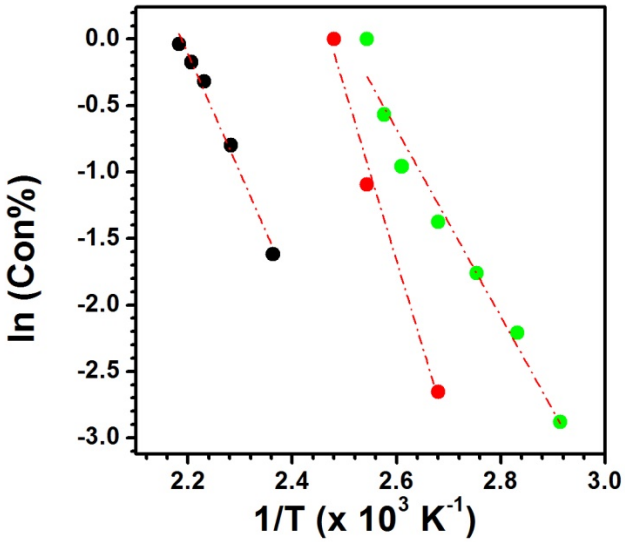

Figure S7. Arrhenius plots for CO oxidation over (E-) $Pd_{25}Cu_{75}$/C (a, black), $Pd_{58}Cu_{42}$/C (b, green), and $Pd_{77}Cu_{23}$/C (d, red) catalysts treated under O_2 at 260 °C for 30 min followed by under H_2 at 200 °C for 30 min.

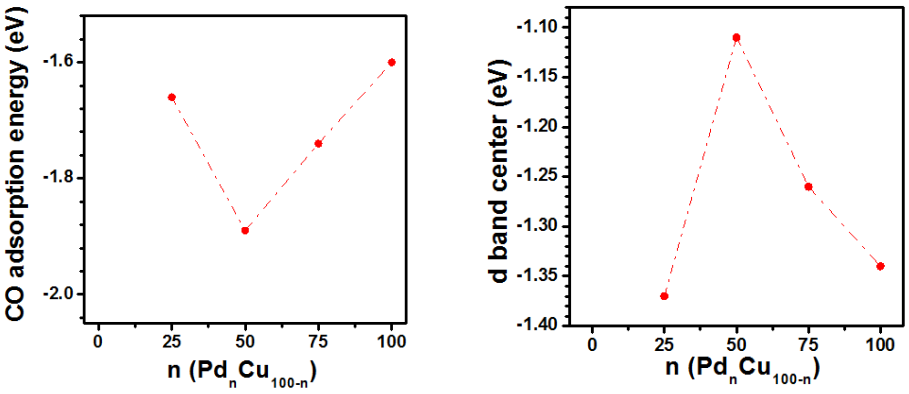

(A) (B)

Figure S8. Plot of calculated adsorption energies (red) (A) and d-band center (B) as a function of binary composition for CO adsorption on models of 4- atom PdCu clusters.

Table S1. XPS peak binding energies (in eV) and relative elemental ratios for PdCu NPs of different compositions (Data pertain to (B-) PdCu NPs).

Catalyst	Condition	Pd 3d	Cu 2p	C1s	O1s	Elemental ratio
$Pd_{21}Cu_{79}$	O_2 –H_2(400 ºC)	341.1, 335.9	932.71, 943.0, 953.9, 962.9	284.76 ($2p_{3/2}$)	533.1, 532.1	21:79
$Pd_{48}Cu_{52}$	O_2 –H_2(400 ºC)	341.0, 335.7	932.44, 952.3	284.8 ($2p_{3/2}$)	532.9, 532.2	60:40
$Pd_{75}Cu_{25}$	O_2 –H_2(400 ºC)	341.2, 335.9	932.2, 952.5	284.76 ($2p_{3/2}$)	533.0, 531.9	81:19

Note: The C 1s peak (284.75 eV) was used as an internal standard for the peak calibration.

Table S2 Fcc type lattice parameter a data and first neighbor distance data for (B-) $Pd_{21}Cu_{79}$/C

Temperature	Fcc type, a (A)	First PDF peak (A)
Room	3.675	2.58
200C	3.698	2.57
400C-1min	3.698	2.57
400C-10min	3.698	2.57
400C-20min	3.697	2.57
400C-30min	3.697	2.60
Back to room	N/A	2.87

Table S3. Comparison of kinetic data of the different PdCu nanoalloy catalysts

Catalysts	d_{NPs} (nm)	ECA (m^2/mg_{Pt}) [a]	Thermal treatment	Reaction rate($\times10^{-6}$ mol/(g_{pd}.s)[b] ($T_{\sim100\%}$)	Ave. D (Dispersion, %)[c]	TOF ($\times10^{-2}$ s^{-1})[d]	E_a (kJ mol^{-1})[f]
Pd	~7.0	25	H_2	2.27*10-5(150)	15	1.52	41.4
B-Pd21Cu79D	7.4±1.2	-	N_2-H_2	6.37*10-5(200)	11	5.90	-
B-Pd48Cu52D	6.0±0.8	-	N_2-H_2	4.85*10-5(155)	18	2.78	-
B-Pd75Cu25D	4.9±0.5	-	N_2-H_2	3.63*10-5(160)	14	2.66	-
B-Pd21Cu79M	7.4±1.2	8.3	N_2-H_2	7.10*10-6(140)	11	0.66	112.6

B-Pd54Cu46M	6.0±0.8	37	N_2-H_2	1.41*10-5(100)	18	0.81	46.2
B-Pd75Cu25M	4.9±0.5	21	N_2-H_2	8.08*10-6(120)	14	0.59	58.5
E-Pd25Cu75M	2.7±0.5	23	N_2-H_2	8.63*10-6(140)	21	0.44	53.2
E-Pd58Cu42M	2.6±0.6	81	N_2-H_2	1.12*10-5(100)	43	0.28	39.6
E-Pd77Cu23M	3.5±0.7	100	N_2-H_2	3.30*10-7(120)	32	0.011	89.7

Note: D is shortened for deep oxidation, where data collected at 300 °C H_2 reduction; while M is shortened for mild oxidation where date collected at 200 °C H_2 reduction. [a] Electrichemically active surface area (ECA) was determined by cycle votammetry. [b]Calculation of reaction rate was based on moles of CO reacted at the flow rate and was normalized against the total mass of Pd in the catalyst. [c]The dispersion of Pd on the surface of one NP was calculated using $D = (6V_m/(a_m\, d)) \times 100\%$, where V_m is the volume of atom Pd, a_m is Pd surface area, and d is the particle size. [d] Calculation of TOF was based on the surface Pd using TOF=Reaction rate/(MW(Pd)×D). Note that the metal loading (20%) is significantly higher than usual (0.1~8%), leading to a higher percentage of buried nanoparticle surface in this work. [d] Data derived from Arrhenius plots (See Figure S8).

Table S4. Calculated adsorption energy, E_{ads} (eV), and d-band center of molecularly adsorbed CO on Pd_4, Pd_3Cu_1, Pd_2Cu_2, Pd_1Cu_3 systems. (Pd: blue dots, Cu: orange dots, C: grey dots and O: red dots)

	Pd4-CO	Pd3Cu1-CO	Pd2Cu2-CO	Pd1Cu3-CO
Model	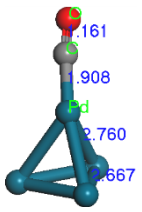	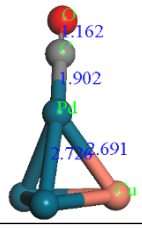	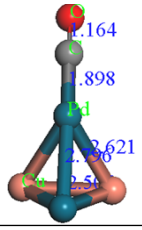	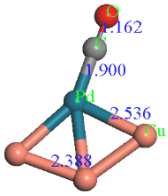
E_{ads} (eV)	-1.60	-1.74	-1.89	-1.66
O-C bond/ Å	1.161	1.162	1.164	1.162
C-Pd bond/ Å	1.908	1.902	1.898	1.900
d-band center /eV	-1.34	-1.26	-1.11	-1.37